Energy Supply Strategy for a Cryogenic Etching by Integrating SMR with Multi Turbine Cooling System Using Joule-Thomson Expansion

Lee Tae Yang [a], Yeongchan Kim[a], Jeong Ik Lee[a*]
[a]*Department of Nuclear and Quantum Engineering N7-1 KAIST 291 Daehak-ro, Yuseong-gu, Daejeon, Republic of Korea*
**Corresponding author: jeongiklee@kaist.ac.kr*

***Keywords: Cryogenic Etching, supercritical CO_2, Small Modular Reactor, Joule-Thomson Expansion**

1. Introduction

A lot of technology has been developed to place transistors closely and uniformly on a horizontal semiconductor plane. Still, because of the limitations involved in stacking transistors flat like that, there's a growing interest in 3D chip stacking. To get vertical etching done effectively, you need to stop etching gases from spreading laterally, which means working at low temperatures to slow down chemical reactions. Plus, by cutting back on the amount of C_4F_8 used for protective film and bumping up the HF ratio, you can speed up the etching process. Unlike traditional etching that happens around 20 °C, creating 3D structures demands cryogenic etching at temperatures between −60 °C and −70 °C [1,2]. Therefore, this study suggests a system that combines a Small Modular Reactor (SMR) with a multi turbine cooling system to power semiconductor manufacturing while also effectively cooling down the heat produced by plasma sources, maintaining those low temperatures.

2. Methods and Results

Semiconductor fabrication facilities need a whole lot of electricity. While traditional setups depend on electricity to operate cooling units, this study proposes a more integrated setup that uses an auxiliary turbine. This design skips the electricity conversion step and directly uses the work from the turbine to drive compressors, allowing for cooling and liquid air production.

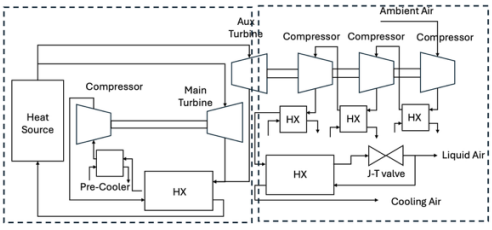

Fig. 1. Overview of the integrated cooling and power generation system for semiconductor fabrication

As shown in Fig. 1, the model developed in this project has two main sections. The first involves the turbine control and branching unit, which manages how steam is distributed between the main turbine that generates electricity and the auxiliary turbine that operates the cooling system. The second part is the integrated cooling and liquefaction unit that converts the mechanical energy from the auxiliary turbine into compressor work to cool down and produce liquified air as a byproduct.

2.1 Multi Turbine Loop Optimization

This approach uses a supercritical CO_2 Brayton cycle to boost thermal efficiency while keeping the design compact. The system splits the flow at the turbine inlet.

The main turbine generates power for the semiconductor fabrication, and the auxiliary turbine provides the mechanical work needed for the compressors in the cooling and air liquefaction cycle.

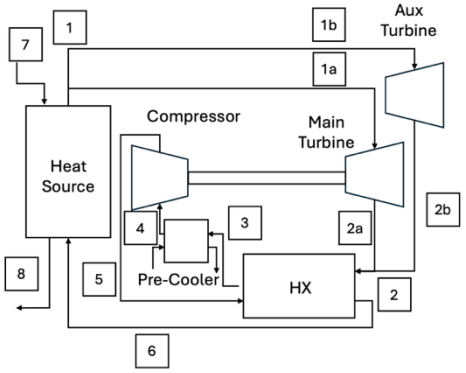

Fig. 2. Design schematic of the multi turbine system loop

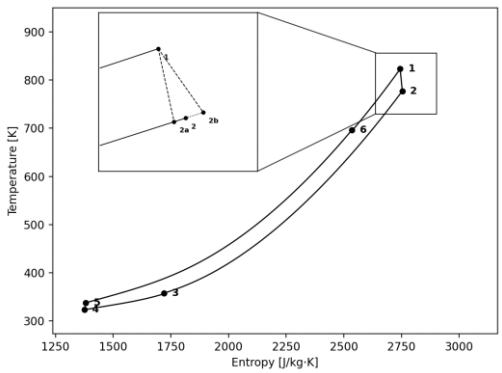

Fig. 3. T-s diagram of the multi turbine system loop

As outlined in Fig. 2, the relationship between temperature and entropy was mapped in the T-s diagram (Fig. 3), and calculations were carried out using our in-house Python code. It was assumed no changes in temperature or pressure at the turbine branching point and set up a balance equation for the Split Ratio (SR), which defines how flow is split between the turbines.

$$h_{2a} = h_1 - \eta_{mainT}(h_1 - h_{2as})$$
$$h_{2b} = h_1 - \eta_{auxT}(h_1 - h_{2bs})$$
$$h_2 = h_{2a} \cdot SR + h_{2b} \cdot (1 - SR)$$

Code utilizes thermodynamic principles to determine the optimal temperature and pressure at each point through iterations, aiming to maximize the overall cycle efficiency for a given SR.

Table I: Thermodynamic Properties (Temperature and Pressure) at Key Points of the Multi Turbine System (SR = 0.6)

Position	Pressure [MPa]	Temperature [°C]
1	19.68	550.00
2	13.49	504.15
3	13.38	84.04
4	13.23	50.00
5	20.00	64.61
6	19.98	423.24

Table I shows the results when 330.00 MW of heat is supplied by the heat source, and the SR for the main turbine is set to 0.6. Under these parameters, the main turbine is able to generate 68.55 MW of power while the auxiliary turbine produces 39.31 MW. The compressor work needed to maintain the Brayton cycle was calculated at 25.25 MW, with a total CO2 mass flow rate of 2110.89 kg/s circulating through the system.

In calculating the efficiency of converting heat from the source into mechanical work from both turbines, we found an overall efficiency of 25.03%. This figure includes the work from the auxiliary turbine (11.91%) that's used for cooling, but the actual efficiency for electricity generation is much lower (13.12%).

2.2 Cooling System with Joule-Thomson Expansion

The liquid air cycle involves extracting heat from ambient air through a series of compression, cooling, and expansion processes. Since nitrogen and oxygen, the primary components of air, can only be liquefied at cryogenic temperatures below −180 °C, the process typically utilizes dried ambient air as the working fluid to ensure operational stability and efficiency across various industrial applications. While utilizing specialized refrigerants may offer superior efficiency and reliability, the primary objective of this study is to propose a novel conceptual framework for a multi turbine cooling system within industrial contexts. Consequently, ambient dry air is selected as the working fluid to demonstrate the feasibility and versatility of this new approach.

The mechanical work generated by the auxiliary turbine is directly used in the series connected compressors of the cooling system. The setup is designed to compress air through compressors and heat exchangers, with air then being expanded via a Joule-Thomson valve [3]. This process helps in separating and collecting liquefied air during isenthalpic expansion, while the leftover chilled air is used for cooling.

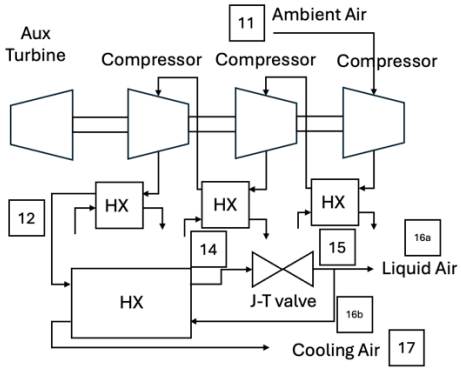

Fig. 4. Configuration of the cooling system connected to the auxiliary turbine

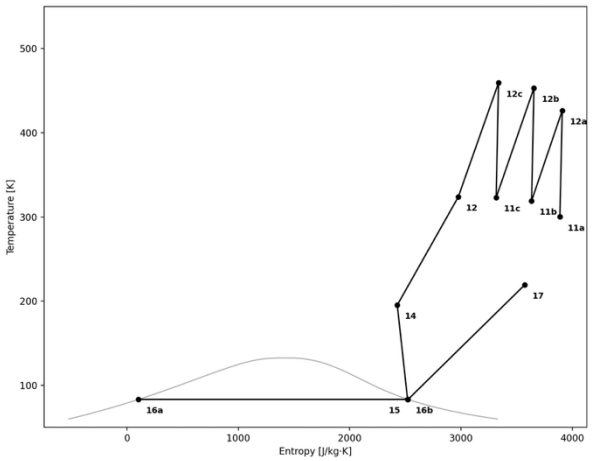

Fig. 5. T-s diagram of the cooling system connected to the auxiliary turbine

Based on the configuration in Fig. 4, we performed thermodynamic calculations using our in-house Python code, which mapped the cycle onto the T-s diagram in Fig. 5. The total work from the compressors was set to match the 39.31 MW of mechanical power from the auxiliary turbine.

For the simulation, we assumed no enthalpy change across the Joule-Thomson valve [4]. Three compressors were configured to work at an identical pressure ratio of 3.19, allowing them to operate efficiently. They consume 12.5 MW, 13.3 MW, and 13.51 MW, respectively, to meet the total power demand of 39.31 MW.

Table II: Thermodynamic Properties (Temperature and Pressure) at Key Points of the Cooling System (total work = 39.31MW)

Position	Pressure [MPa]	Temperature [°C]
11	0.101	27.00
Comp A	0.323	153.23
HX A	0.303	45.99
Comp B	0.967	180.03
HX B	0.947	49.99
Comp C	3.021	186.17
HX C	3.001	50.68
12	3.001	50.68
14	2.981	-77.80
15	0.121	-189.88
17	0.101	-53.77

Table II provides the temperature and pressure values at each point in the cooling system using the 39.31 MW from the auxiliary turbine. Our in-house code calculates total work by deriving enthalpies based on the temperature and pressure at each state point after defining the target cooling capacity. The cooling capacity was adjusted iteratively to ensure that the turbines' total work equaled 39.31 MW, leading to a total heat removal rate of 7.96 MW. The Coefficient of Performance (COP), which measures heat removed against mechanical work input from the auxiliary turbine, came out to be 0.27.

This value is relatively small compared to the 39.31 MW of compressor work. Instead of using common industrial refrigerants like ammonia or hydrocarbons, we opted for air with lower specific heat and density for the cooling process. This choice results in a much higher mass flow rate, which in turn causes the low COP of 0.27. Most of the energy input goes toward liquefying the air rather than direct cooling. Out of a total airflow rate of 98.12 kg/s, only 0.17 kg/s turns into liquefied air.

In practice, the production of dry clean air for use as a refrigerant incurs significant operational costs. These costs primarily stem from auxiliary processes, such as purge losses and thermal energy consumption during the regeneration phase. However, the COP presented in this study represents an ideal value, calculated by excluding the secondary costs associated with the air purification and drying processes.

3. Conclusions

As semiconductor fabrication rapidly advances, energy demands are soaring. Especially, 3D semiconductors, devised to overcome the physical limitations of placing transistors on a planar surface, represent a groundbreaking technology. However, implementing this technology requires the generation of sufficient electrical energy for the manufacturing process while simultaneously maintaining the extremely low temperatures necessary for cryogenic etching. To enhance energy management, designed system has features a multi turbine layout within the SMR, where the main turbine focuses on electricity generation while the auxiliary turbine handles the cooling part.

Rather than running a cooling system powered by conventional electricity, directly leveraging the compressor work for cooling was chosen to improve efficiency. This system comes with the flexibility to adjust design according to different working fluids and cycles, making it adaptable to specific semiconductor fabrication facilities.

In this study, ambient air was used as the working fluid simply as a baseline case. However, it is expected that a higher COP could be achieved by adopting an optimized working refrigerant suitable for practical semiconductor facility applications, as well as by considering the required cooling temperature range and diversifying the cooling methods. Such improvements will enable a direct quantitative comparison against conventional cooling infrastructures. Furthermore, the proposed multi turbine cooling architecture holds significant potential for diverse industrial applications, particularly in managing the intensive thermal loads generated by GPU clusters in AI data centers.

ACKNOWLEDGEMENT

This work was supported by the National Research Foundation of Korea (NRF) grant funded by the Korea government (MSIT) (No. : RS-2024-00436693).

REFERENCES

[1] M. J. de Boer, J. G. E. Gardeniers, H. V. Jansen, E. Smulders, M. J. Gilde, G. Roelofs, J. N. Sasserath, and M. Elwenspoek, Guidelines for Etching Silicon MEMS Structures Using Fluorine High-Density Plasmas at Cryogenic Temperatures, Journal of Microelectromechanical Systems, Vol. 11, No. 4, pp. 385-401, August 2002.

[2] K. Kim, Cryogenic Etching in Advanced Electronics Manufacturing: Applications and Challenges, Applied Science and Convergence Technology, Vol. 33, No. 6, pp. 161-170, November 2024.

[3] T. A. Howe, A. G. Pollman, and A. J. Gannon, Operating range for a combined, building-scale liquid air energy storage and expansion system: energy and exergy analysis, Entropy, Vol.20, p. 770, 2018.

[4] M. Kılıç and A. F. Altun, Comprehensive Thermodynamic Performance Evaluation of Various Gas Liquefaction Cycles for Cryogenic Energy Storage, Sustainability, Vol.15, p. 16906, 2023.

[5] ASHRAE, Thermal Guidelines for Data Processing Environments, 5th ed., ASHRAE, Atlanta, 2021.

[6] Y. Kim, S. Choi, and J. I. Lee, Application of Open-Air Brayton Cycle to sCO2-cooled KAIST Micro Modular Reactor, Transactions of the Korean Nuclear Society Spring Meeting, May 18-19, 2023.

[7] D. H. Kim, S. Oh, Y. J. Chae, and J. I. Lee, Supercritical steam Rankine cycle design optimization for molten salt reactor application, Annals of Nuclear Energy, Vol.181, p. 109498, 2023.